Base Surface Definition for the Morphometry of the Ear in Phantoms of Human Heads

J. Márquez Flores[1], I. Bloch[2,] F. Schmitt[2]
[1]Image and Vision Lab, CCADET, UNAM, P.O. Box 70-186, México, D.F., 04510
[2]TSI Dept., Ecole Nationale Supérieure des Télécommunications, 46 rue Barrault, 75634 Paris, France.

Abstract— **To assess ear thickness and other features of human heads, we defined a reference surface that interpolates the head shape in the region of interest. Laser-scan acquisitions were obtained from real human heads and processed for the construction of anthropomorphical phantoms, originally used for dosimetry studies of hand-held mobile phones. Raw data was converted to cylindrical range images and several image processing techniques were then applied for 3D-model construction. A triangulated surface was then obtained for rendering, and for CAD and finite-element simulations. The ear region was then isolated and replaced by a Coons patch surface that interpolates the skull, using the range-image information around the ear. A baseline surface was thus defined, useful for measuring features of human heads; in particular, an average thickness of the ear was estimated on 41 individuals. Head models "with" or "without" ears were then built for assessing dosimetry and anthropometry problems.**

Keywords— **Anthropometry, head shape, ear thickness, Coons patches, surface interpolation.**

I. Introduction.

Besides phone terminal positioning and other variables, radio-frequency wave absorption by the human body head depends on anatomical complex features, in particular at the ear and mouth regions. Homogeneous phantoms have been previously used [1], and accuracy improvements up to 2 mm precision resolution from MRI (*Magnetic Resonance Imaging*) scans have been made [2]. However, these studies are based on a single morphological average from army anthropometrical data from male subjects, not representative of the population of mobile phone users. Individual head models from 3D laser-scan acquisitions of human subjects will allow simulation of power absorption in anthropomorphic phantoms of several subjects.

In general, measurement of morphological features on human heads requires a proper spatial frame of reference. Ear thickness, in particular, can been defined by 3D plane fitting, and the ear has be replaced by a lossless spacer of 4mm in SAR studies on head phantoms [3]. Besides the overestimation of the ratio between energy absorbed in the ear and the rest of the head, a more natural approach would be the building of phantoms "without ears", or with a generic ear shape, as in the SAM (Standard Anthropometry Model [4]). Regarding anthropometrical applications, the plane orientation turns out to be very sensitive to head-shape variations, the choice of the reference points, and comparisons of thickness or other measures in several individuals, prompts for common frames of references, such as the head itself [5]. In fact, the answer of simple questions such as what is the length of the nose, or the thickness of the ear depends on defining an imaginary base surface where the nose or the ear "begins".

In the present paper, we present a novel approach, using a fitting Coons patch, which interpolates the skull surface in the ear region, and may be used to interpolate the zone underlying other features, and replace them with a 3D curved patch. Once interpolated, the ear, the nose or other features can be subtracted, in order to obtain morphological measures with respect to a reference surface, or to make inter-individual comparisons, morphological averages and other analysis.

II. Materials and Methods

A. Laser-scan acquisition protocol.

The numerical acquisition of human heads was performed with a 3D laser scanner from *Cyberware* [6]. Fig. 1 shows the acquisition setup, with physical landmarks to reproduce the same position for all subjects. The scanner rotates around the head axis, producing distance information of the 3D relief. Two 3D renderings of sample phantoms are also shown at right. In total, 41 subjects were scanned, with 12 women in the final sample.

Fig. 1. Laser scan acquisitions of 41 people. At right, two renderings of the triangular mesh models in *VRML* format.

Raw acquisition data consists of meridian profiles, with varying number of points, depending on relief. Spacing Δy between points is less than 1mm in height **y** projection, and less than 0.5 mm in angular position θ. Depth differences $\Delta\rho$ may vary widely (several millimeters), specially at the skullcap, under the chin and behind the ears.

B. Cylindrical range-image processing

Before model construction, several pre-processing operations were performed. Floating range images of 480×580×5-byte resolution were extracted from the raw scan data, in order to filter out artifacts and noise, preserving accuracy, and locate morphological features in *image space* and then in *object space*. The range-image representation is also convenient for other manipulations and measurements, since 3D information is displayed in the *Mercator cylindrical projection* as a gray-level image, as shown in Fig. 2, where the relations between coordinates systems are explained.

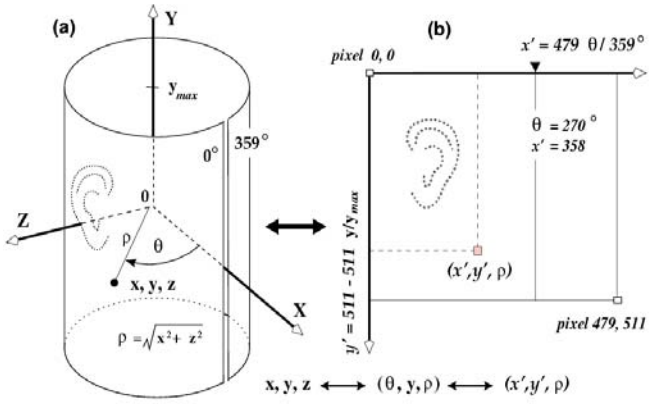

Fig.2. (a) Object-space coordinates and its projection during laser-scan acquisition. (b) Range-image space coordinates (512 × 480 pixels in floating point precision). Meridian θ=27° (column x'=358) is the starting/ending meridian for acquisition.

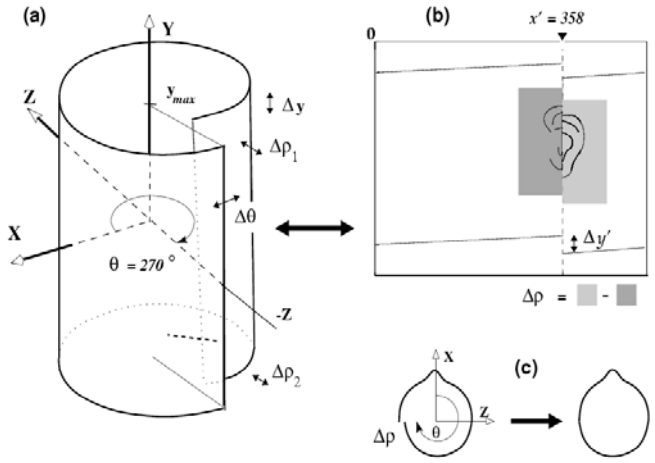

Fig.3. (a) Helicoidal registration mismatch. (b) On the range-image projection the mismatch is evident at the closing meridian. The range component $\Delta\rho$ appears as a gray level mismatch. (c) shows a progressive correction of the $\Delta\rho$ component.

Phantom construction (triangular meshing) includes format conversions and image processing techniques, applied to range images, where gray level codes depth (or height, from the rotation axis of the head). Restoration of missing data or artifact removal employed also the interpolated surface described in the next section.

Since there may be alignment mismatches between starting and ending acquisition meridians, a special procedure called helicoidal mismatch correction was developed to incrementally correct each contour in order to match the initial and final meridians. Fig. 3 shows the helicoidal mismatch in the general case.

Further processing of range images is detailed in references [6, 7]. Interactive 3D visualization of mesh models is done in the VRML (*Virtual Reality Modeling Language*) format, as illustrated in Figs. 5, 6 and 8.

C. Specific extraction and manipulation of the ear region.

A boundary rectangular zone around the ear was used to build a reference surface that interpolates the head shape in this zone. Using first-order surface fitting, the simplest approximated patch to replace the ear structure was a Bilinearly Blended Coons patch [8, 9], which interpolates the surface solely from the boundary information and corners of the reference surface, as illustrated by Fig. 4.

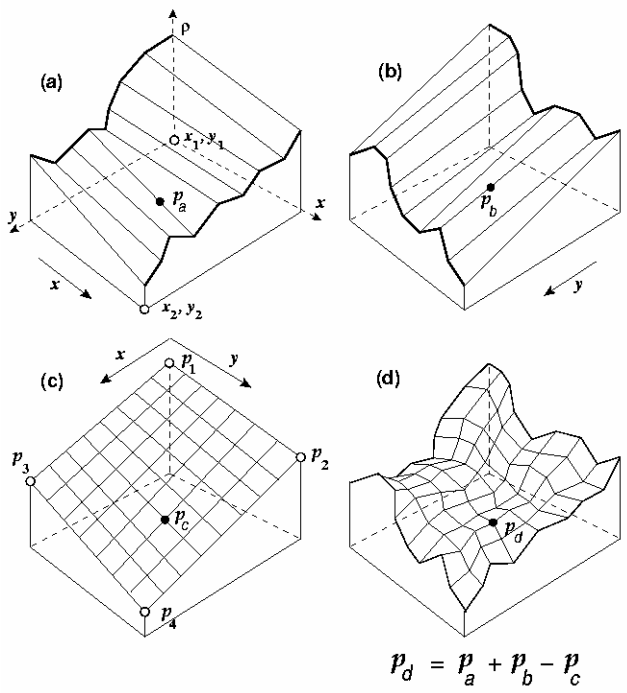

Fig. 4. Construction of a bilinearly-blended Coons patch by (a) and (b): orthogonal lifting of boundary information of a rectangular ROI. It is then combined with (c): the bilinear fitting plane defined by the ROI corners. (d) Shows the resulting patch.

The construction method combines orthogonal lifting of bounding contours and a standard bilinear interpolator using the 4 corners of the ROI, obtaining, by cross modulation, the

spline surface resulting from a tensor product of the bounding contours, first in the *X* direction, then in the orthogonal *Y* direction. This surface is also known as an "implicit surface", and higher-order splines can be also used.

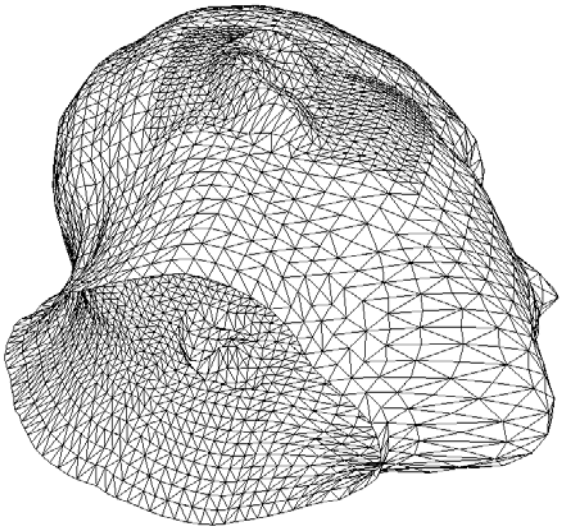

Fig. 5. A 3D-rendering of the triangular mesh model with finer resolution in the ear region.

III. Tests and results

The resulting surface interpolates the cranium at the ear region, preserving shape, and a gradual smoothing of the ear can be achieved by blending from 0.0 (no ear) to 1.0 (detailed ear), without modifying other regions of the head phantom. This reference surface serves also to define a non-planar baseline for thickness estimations of the ear at various locations with respect to the head, as shown later in Fig. 9. Negative heights correspond to regions under this surface, intruding into the head. The ear structure in Fig. 5 is thus subtracted and isolated, as shown in Figs. 6 to 8.

Fig. 6. Isolation and filtering of the ear zone by interpolation with a bilinearly-blended Coons patch on the cylindrical range image.

An application of the database consisted in the construction of a robust morphological average of the human ear over a subset of the database. The methods are presented elsewhere [10]. We only mention that the present approach also permitted averaging of the implicit surface that interpolates the skull. Thus, a morphological-average of the head "without ears" can be obtained, too.

The average thickness of the ear in 41 individuals was defined as the average height, using several criteria for statistical measures from sample regions inside the ear.

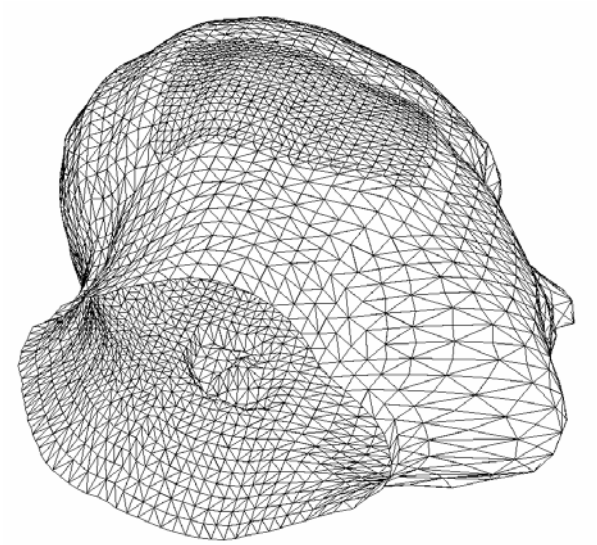

Fig. 7. Same as Fig. 5, with the ear structure replaced by the interpolated surface inside the high-resolution patch.

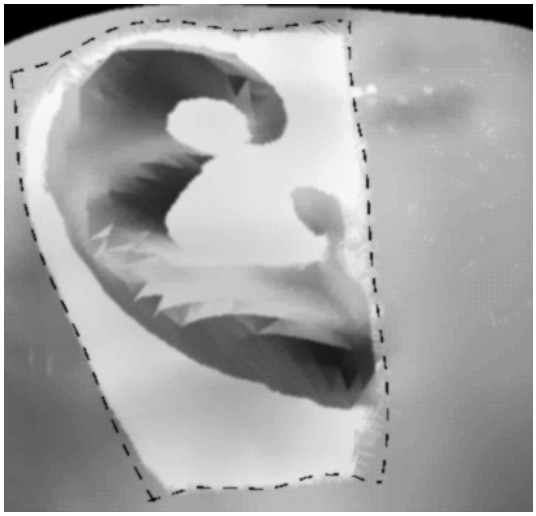

Fig. 8. Superposition of the head surface before (dark gray) and after (light gray) ear filtering. The light-gray ROI is the interpolated "implicit" surface.

Fig. 9 summarizes these measures. Fig. 10 shows an histogram of the parameter $\langle C \rangle - \langle A+E \rangle/2$, where *A* to *E* represent sampled ROI heights as shown on Fig. 9, and $\langle * \rangle$ denotes the average height in those ROI's. Finally, Fig. 11 illustrates the construction of morphological averages of the ear and its implicit base surface, integrated to a generic head phantom (virtual as well as physical) for dosimetry studies.

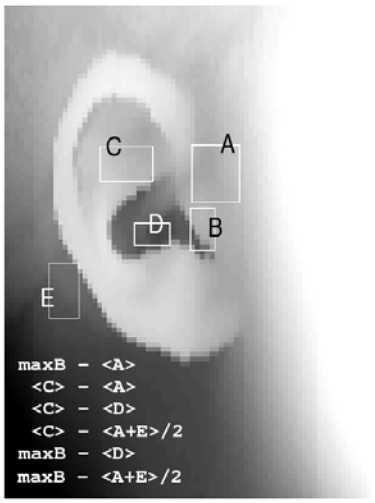

Fig. 9. Height and depth morphometry on different ear zones for the estimation of average thickness. The Coons patch is the baseline surface.

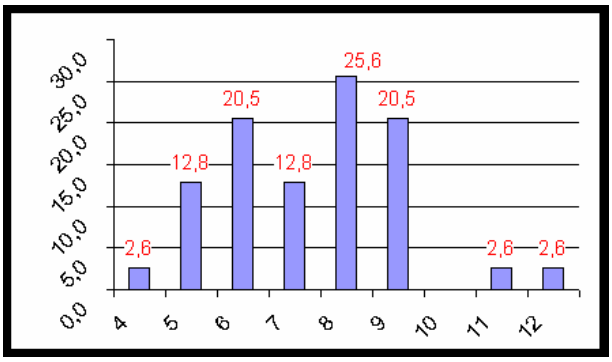

Fig. 10. Histogram of estimated height <C> - <A+E>/2, in 12 classes from 41 individuals. Height units are in mm.

IV. Conclusion

A database of 41 human head profiles was built and a base surface was obtained from boundary information at the ear region, using *bilinearly-blended Coons patches*. This interpolated surface was used in five applications: (1) to remove artifacts and to restore the shape of the head, (2), to define a reference for height measures of any head or facial feature, (3), to isolate and filter the ear structures, (4) to build head phantoms without ears, and (5) to obtain morphological averages of the ear and the implicit surface that interpolates the head shape at the ear region.

Acknowledgment

The present work resulted from collaboration between the *Ecole Nationale Supérieure des Télécommunications*, Paris, and *the Alcatel Corporate Research Center, (Marcoussis laboratories).* We gratefully acknowledge the assistance of Dr. M. Nahas, from the Paris VII University.

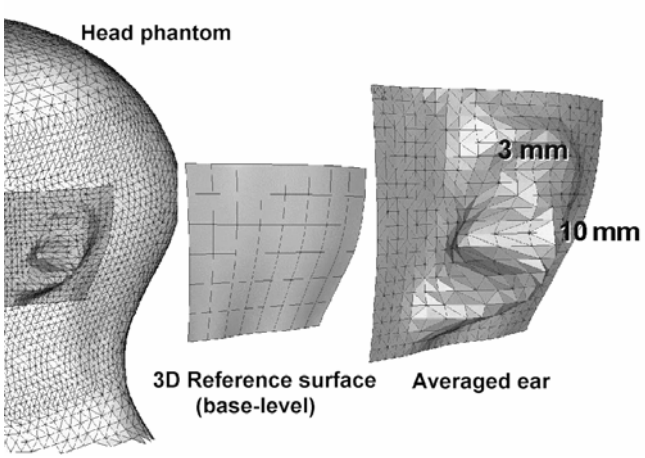

Fig. 11. Construction of an average anatomical feature (the ear of 41 individuals) for integration to a generic phantom.

References

[1] C. Grangeat et al., "Radio-frequency radiation from mobile phones", *Alcatel Telecommunications Review,* 4th Quarter 1998, pp.298-304.

[2] J. Wiart et al., "Calculation of the power deposited in tissues close to handset antenna using non uniform FDTD", Proceedings of the *Second World Congress for Electricity and Magnetism in Biology and Medicine,* Bologna, June 97, Plenum Press.

[3] M. Burkhardt and N. Kuster. "Appropriate modeling of the ear for compliance testing of handheld MTE with SAR safety limits at 900/1800 MHz." *IEEE Transactions on Microwave Theory and Techniques,* Vol. 48, No. 11, 2000, pp 1927-1834.

[4] - "SAM - the Standard Anthropomorphic Model", Phantom specification at: http://www.sam-phantom.com/MCL_SAM.pdf. Information at: http://www.sam-phantom.com/SAMinfo.htm.

[5] V. F. Ferrario, Ch. Sforza, V. Ciusa. G. Serrao and G. M. Tartaglia. "Morphometry of the normal human ear: A cross-sectional study from adolescence to mid-adulthood." *Journal of Craniofacial Geneticas and Developmental Biology,* 19, pp. 226-233

[6] Inc. Cyberware Laboratory, "4020/rgb 3d scanner with color digitizer", available information at the internet address: http://www.cyberware.com/pressReleases/index.html, 1990.

[6] J. Márquez, I. Bloch and F. Schmitt. "IPCYL : Logiciels de traitement de données cylindriques et images en profondeur, MakeTri et Voxelize: maillage triangulaire et voxelization pour la création de fantômes antropométriques". Description des méthodes et documentation des logiciels (Vers. 1.0). *Dept. IMAGES, ENST,* Paris, october 1999.

[7] J. Márquez, T. Bousquet, I. Bloch, F. Schmitt and C. Grangeat. "Laser-Scan Acquisition of Head Models for Dosimetry of Hand-Held Mobile Phones". Poster # 25, *BioElectroMagnetics Society, 22th Annual Meeting,* Technical University, Munich, Germany. Abstract Book (Technical University, Munich): pp. 123. June 9-16, 2000.

[8] S.A. Coons. Surfaces for computer-aided design of space forms, MIT, *Project MAC,* Tech. report TR-41, MIT, Cambridge, Mass., June 1967.

[9] R. Barnhill, "Coons patches and convex combinations", in Les Piegl, editor. *Fundamental Developments of Computer Aided Geometric Modeling*. Academic Press, London, 1993.

[10] J. Márquez, I. Bloch, T. Bousquet, C. Grangeat and F. Schmitt. "Morphological Robust Average of the Ear Shape of Human-Head Phantoms". *Unpublished*. 2003.